

# Modeling individual-specific human optic nerve head biomechanics. Part II: influence of material properties

Ian A. Sigal · John G. Flanagan · Inka Tertinegg ·  
C. Ross Ethier

Received: 12 April 2007 / Accepted: 29 January 2008 / Published online: 27 February 2008  
© Springer-Verlag 2008

**Abstract** Biomechanical factors acting within the optic nerve head (ONH) likely play a role in the loss of vision that occurs in glaucoma. In a companion paper (Sigal et al. 2008), we quantified the biomechanical environment within individual-specific ONH models reconstructed from human post mortem eyes. Our goal in this manuscript was to use finite element modeling to investigate the influence of tissue material properties on ONH biomechanics in these same individual-specific models. A sensitivity analysis was carried out by simulating the effects of changing intraocular pressure on ONH biomechanics as tissue mechanical properties were systematically varied over ranges reported in the literature. This procedure was repeated for each individual-specific model described in the companion paper (Sigal et al.

2008). The outcome measures of the analysis were first and third principal strains, as well as the derived quantity of maximum shear strain, in ONH tissues. Scleral stiffness had by far the largest influence in ONH biomechanics, and this result was remarkably consistent across ONH models. The stiffnesses of the lamina cribrosa and pia mater were also influential. These results are consistent with those obtained using generic ONH models. The compressibility of the pre-laminar neural tissue influenced compressive and shearing strains. Overall, tissue material properties had a much greater influence on ONH biomechanics than did tissue geometry, as assessed by comparing results between our individual-specific models. Material properties of ONH tissues, particularly of the peripapillary sclera, play a dominant role in the mechanical response of an ONH to acute changes in IOP and may be important in the pathogenesis of glaucoma. We need to better understand inter-individual differences in scleral biomechanical properties and whether they are clinically important.

---

Ian A. Sigal now a post-doctoral research fellow at Ocular Biomechanics Laboratory, Devers Eye Institute, Legacy Health Research, Portland, OR, USA. (isigal@deverseye.org).

---

I. A. Sigal · C. R. Ethier  
Department of Mechanical & Industrial Engineering,  
University of Toronto, Toronto, Canada

I. A. Sigal · C. R. Ethier  
Institute for Biomaterials and Biomedical Engineering,  
University of Toronto, Toronto, Canada

J. G. Flanagan · I. Tertinegg · C. R. Ethier  
Department of Ophthalmology and Vision Sciences,  
University of Toronto, Toronto, Canada

J. G. Flanagan  
School of Optometry, University of Waterloo, Waterloo, Canada

C. R. Ethier (✉)  
Department of Bioengineering, Imperial College London,  
London SW7 2AZ, UK  
e-mail: r.ethier@imperial.ac.uk

**Keywords** Biomechanics · Glaucoma · Optic nerve head · IOP · Finite elements · Strain · Sclera · Lamina cribrosa

## 1 Introduction

This paper is the second in a two-part series in which we consider the biomechanics of the optic nerve head (ONH) and its role in glaucoma. Readers are referred to the first paper in the series (Sigal et al. 2008) for background material and the motivation for studying ONH biomechanics.

In the first paper (Sigal et al. 2008) we used individual-specific models constructed from post mortem human eyes to investigate the biomechanical environment within the ONH

by finite element modeling. One of the questions asked in that paper was what effect inter-individual geometric (anatomic) differences have on ONH biomechanics. This question is important because clinical data show that patients can have very different susceptibility to elevated IOP; the source of this differing susceptibility is unknown. To answer this question we used the same set of tissue mechanical properties for all ONH models, and observed only modest differences in strains within the ONH between models. In view of this result, it is appropriate to ask if other individual-specific factors could cause differences in the biomechanical environment within the ONH.

In a previous study (Sigal et al. 2005a) we carried out a sensitivity analysis, considering the relative influences of 21 input factors on ONH biomechanics. It was found that scleral properties, particularly scleral stiffness, had a very large influence on ONH biomechanics, suggesting that tissue properties are likely an important factor driving inter-individual differences in ONH biomechanics. However, this previous work relied on generic (i.e. non-individual-specific) models of the ONH, and it is important to determine if similar conclusions would be drawn if more physiologically realistic individual-specific models were used.

The purpose of this manuscript is to analyse the sensitivity of ONH biomechanics to the mechanical properties of the ONH tissues using individual-specific models. By comparing the results of this study with those in the companion paper (Sigal et al. 2008), it was also possible to determine whether the effects of geometry depend on the material properties, and to compare the relative influences of geometry and material properties on ONH biomechanics.

## 2 Methods

A sensitivity analysis was carried out based on individual-specific models reconstructed from ostensibly healthy human optic nerve heads, using a finite element modeling approach similar to that described previously for use with generic axisymmetric models (Sigal et al. 2005a). In brief, input factors were systematically varied and their effects on ONH biomechanics were assessed through the resulting variations in a set of “outcome measures” that quantified the biomechanical environment in the ONH. The models were the same ones described in the companion paper (Sigal et al. 2008). Eyes were obtained and managed in accordance with the provisions of the Declaration of Helsinki for research involving human tissue. The details of model construction and boundary condition application were identical to those described in the companion paper (Sigal et al. 2008).

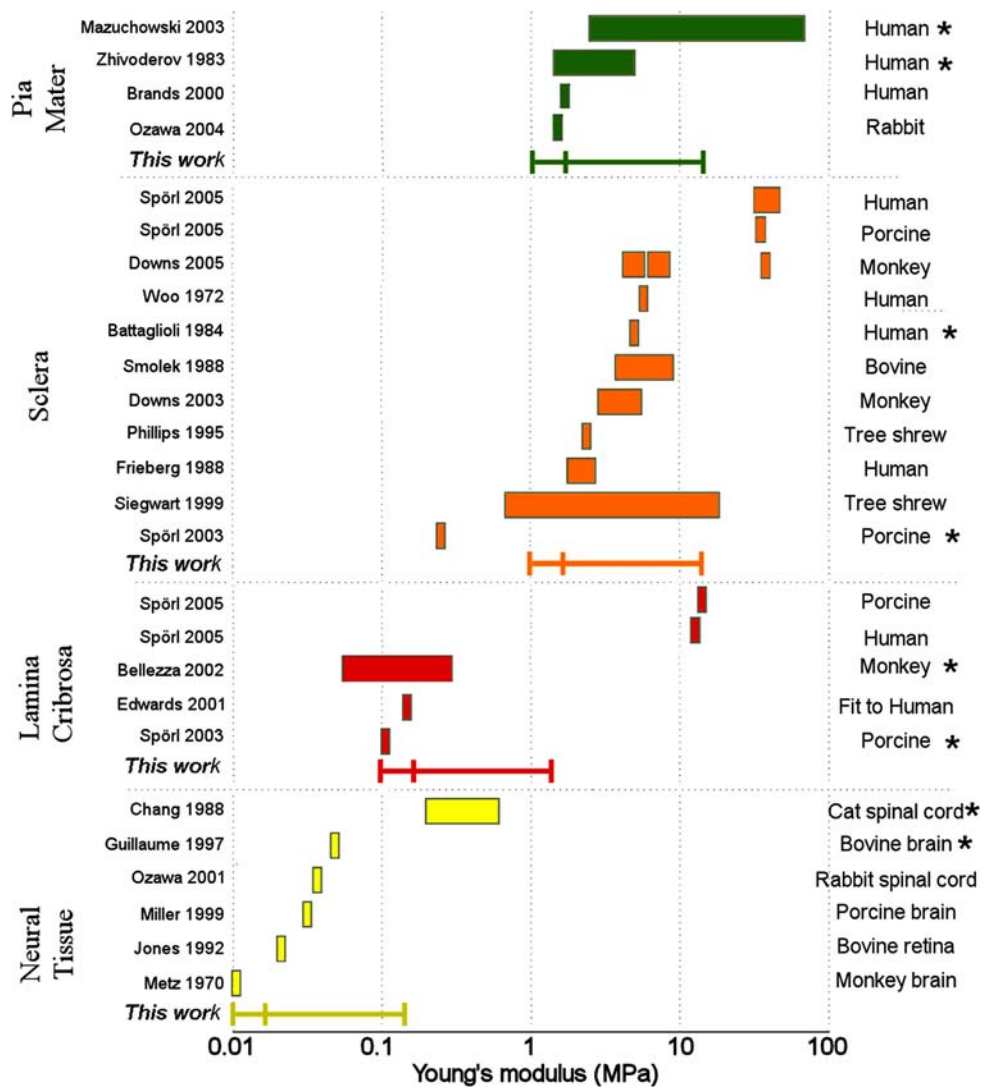
### 2.1 Input factors

The input factors that were varied in this analysis were the material properties of the various ONH tissue regions. A “baseline” combination of material properties was defined (see below for details), and then for each model we systematically varied each input factor independently to determine how the input factors influenced ONH biomechanics. All the tissues were assumed linearly elastic and isotropic, and, except for the pre-laminar neural tissues, also incompressible. Therefore ONH biomechanical behaviour was completely defined through six input factors: the stiffness (Young’s modulus) of each of the five tissue regions, and the compressibility (Poisson ratio) of the pre-laminar neural tissue. Input factor baseline values and ranges were defined based on available literature (Sigal et al. 2005a). Unfortunately, the actual range of admissible (physiologic) values for the input factors is known only approximately for some factors (Fig. 1). Obviously, if an input factor was allowed to vary over an unnaturally large range, it could increase variations in the outcome measures, and the influence of the input factor would be over-estimated. To avoid this problem we followed an approach similar to that in Sigal et al. (2005a), in which we allowed Young’s modulus values to vary over proportionally comparable ranges, with all five moduli varying from 1/3 to 4 times the baseline values. The compressibility of the pre-laminar neural tissue was varied from practically incompressible (Poisson ratio of  $\nu = 0.49$ ) to a relatively low value of 0.39. Studies of brain tissue compressibility have found it to be “nearly incompressible” (Edwards and Good 2001). The lower values of the Poisson ratio allowed in this study are intended to model the changes in vascular volume within the pre-laminar neural region and in axoplasmic flow that may occur as IOP is varied.

Finite element simulations were carried out at 12 equally spaced steps over the input range for the modulus of elasticity of each tissue region, and 11 equally spaced steps over the input range for the compressibility of the pre-laminar neural tissue. This is slightly fewer steps than were used in a previous study (Sigal et al. 2005a), since the CPU time per step was much larger. Comparison of plots of effects of outcome measure as a function of input factor level between this study and the one in Sigal et al. (2005a) suggests that this number of steps was sufficient to capture the essential features of the response.

Finite element simulations were therefore carried out for 726 cases: 10 individual-specific and one generic model, each solved at a baseline level plus 11 variations of each of 5 material properties and 10 variations of pre-laminar neural tissue compressibility. All models were meshed according to the results of the mesh refinement study described in Sigal et al. (2005b). Details of the model meshes are provided in Sigal (2006). Solutions were obtained using Ansys v8.1

**Fig. 1** Summary of the magnitude of Young's moduli reported in the literature for the tissues of the ONH: pia mater (green), sclera (orange), lamina cribrosa (red) and neural tissue (yellow). Each row is a literature reference, with the reported range of values shown by the horizontal bars. Bars with asterisks were cases where Young's modulus was not directly reported but could be computed from other reported data, as described in Sigal (2006). The species/tissues on which the measurements were performed are shown on the right. Also shown are the ranges of modulus used in this work (vertical lines represent minimum, baseline and maximum levels). Note the logarithmic scale for the modulus. For Downs et al. (2005), the three magnitudes shown are for (from left to right) equilibrium on normal eyes, equilibrium on early-glaucomatous eyes, and instantaneous on both types of eyes



(ANSYS Inc., Canonsburg, PA, USA) PCG solver with default parameters. Each solution required approximately 40 min (wall clock time) using a dedicated desktop workstation with Windows XP SP1, an Intel 3.0GHz CPU and 4 GB of memory. As described in Sigal et al. (2005b, 2007b), solutions were ported from Ansys to Amira 3.1.1 (Mercury Computer Systems, USA) for post-processing.

### 2.2 Outcome measures

Changes in IOP produce complex deformations of the ONH, where the tissues are subject concurrently to various modes of strain. Because strain is believed to be the biomechanical factor that influences cellular physiology in ONH tissues, we have focussed on strain as an outcome measure. More specifically, we analyzed three modes of strain: tension (first principal strain), compression (third principal strain) and shear (maximum shearing strain). Maximum shear strain was

computed as the average, in absolute magnitude, of the first and third principal strains, as described in (Sigal et al. 2007b, 2008). The distribution of the magnitude of each strain mode, on each tissue region of each model, was computed using the method described in Sigal et al. (2007b). From these distributions the values of the 50th and 95th percentiles were computed, to represent the median and peak levels of the strain mode within that tissue. A model response was therefore characterized by 30 outcome measures: median and peak levels of three modes of strain within each of the five tissue regions.

For each model, a region of interest (ROI) was defined based on the geometry of the anterior surface of the lamina cribrosa, as described in Sigal et al. (2007b) and in the companion paper (Sigal et al. 2008). Since the ROI was defined at the reconstructed IOP, there was no need to update the ROI as the material properties varied. Details of the ROI for all the models used in this study can be found in Sigal et al. (2007b).

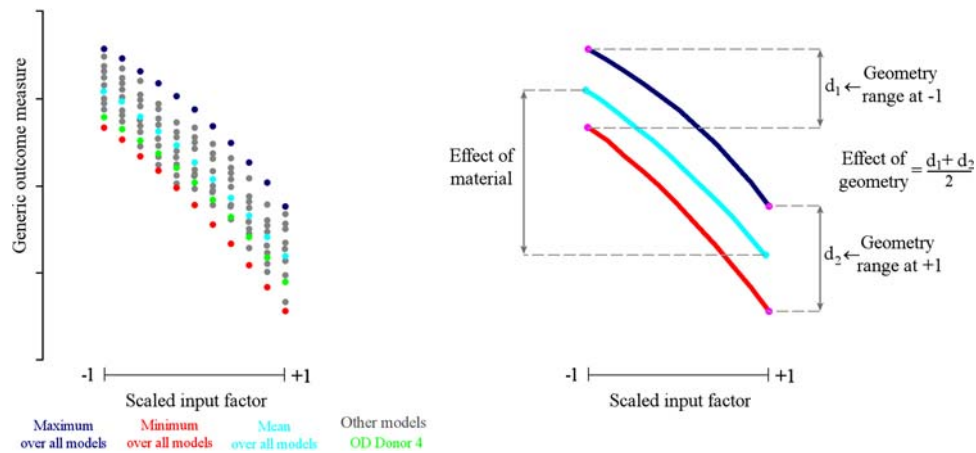


**Fig. 2** Schematic diagram to illustrate the definition of parameters used to quantify the influences of geometry and material properties. The plots show a generic outcome measure versus a generic input factor; here the input factor is scaled so that its minimum and maximum values are  $-1$  and  $+1$ . Each point on the left panel is a response for a particular individual-specific model, colored according to whether the point is the maximum (dark blue) or minimum (red) over all individual-specific models for the specific input factor level. Also shown is the average response across all individual-specific models used to compute the effect of material (light blue). To illustrate the response from one

individual-specific model, all responses of one eye (right eye, OD, of donor 4) are coloured green. The grey points represent responses for other eyes that were neither the maximum nor minimum response for that specific factor level. The average of the geometry ranges at the minimum ( $-1$ ) and maximum ( $+1$ ) levels of an input factor were then defined as the *effect of geometry*. The *effect of material* was defined as the variation of the average for all individual-specific models across the range of input factor values. For clarity we also show on the right panel lines formed by joining the maximum (dark blue line), minimum (red line), and average (light blue line) points

### 2.3 Analysis of input factor influence and outcome measure sensitivity

A systematic approach analogous to that described in Sigal et al. (2005a) for generic models was then used to determine the sensitivity of the 30 outcome measures to the 7 input factors for the 726 cases studied. More specifically, we computed the *absolute response* of an outcome measure to a single input factor as the range (maximum – minimum) of the outcome measure values while varying only that input factor. For each outcome measure we then summed its absolute responses to all input factors to obtain the outcome measure's *total response*. Since all outcome measures studied here are strain modes, their values could be compared directly and there was no need to compute a relative response, as in Sigal et al. (2005a). A global view of the importance of an input factor was obtained by adding the absolute responses of a single input factor over a set of outcome measures, which was defined as that input factor's *total influence*.

### 2.4 Response envelopes, effect of geometry and effect of material

Because each of the ten individual-specific ONHs used in this study had a different geometry, comparison between the models gives an indication of the effects of geometry. Such a comparison, when combined with the results of varying tissue material properties, allowed us to evaluate the relative

importance of model geometry and material properties using the following approach. For a given outcome measure there were ten responses, one for each individual-specific model at each value of an input factor (grey points in Fig. 2). From the responses of all individual-specific models three quantities were computed at each input factor level: maximum, minimum and average (dark blue, red and light blue points, respectively in Fig. 2). The difference between the maximum and minimum values was named the *geometry range* at that specific input factor level. The geometry range represents the variation in the outcome measure as a result of differences in geometry (anatomy) between models. If all individual-specific models produced the same outcome measure at an input factor level the geometry range for that input factor level would be zero. The average of the geometry ranges at the minimum ( $-1$ ) and maximum ( $+1$ ) levels of an input factor were then defined as the *effect of geometry*. Similarly, the *effect of material* was defined as the variation of the average for all individual-specific models across the range of input factor values. If variations in an input factor had no effect on the outcome measure levels, then the lines in Fig. 2 would be horizontal and the effect of material would be zero. When the changes in outcome measure due to variations in an input factor were monotonic, as in Fig. 2, the highest and lowest averages were at the extreme input factor levels ( $-1$  and  $+1$ ).

Finally, to describe the relative influence of material properties and geometry, we computed the *ratio of effect of*

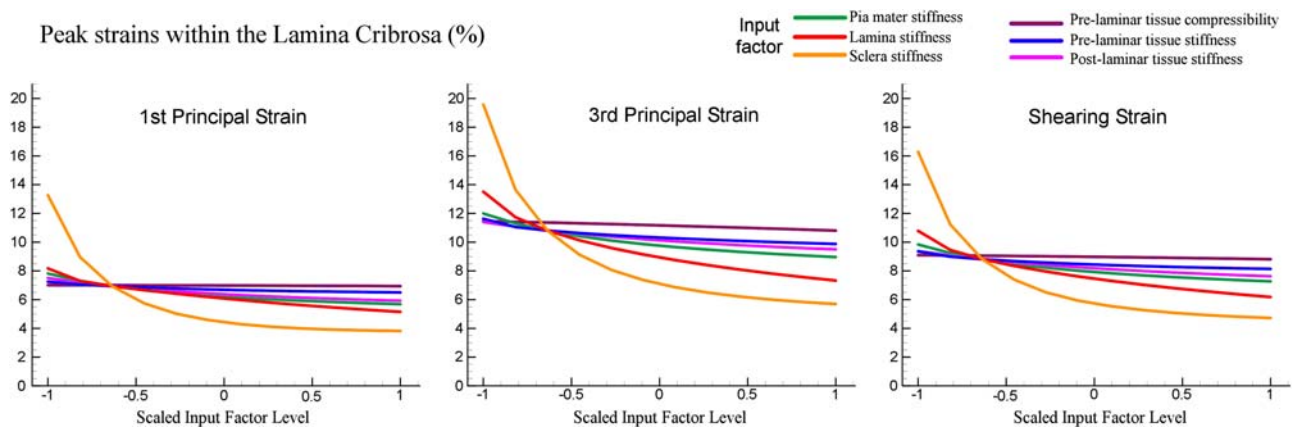


**Fig. 3** Sensitivity to variations in all input factors of peak tensile strain (left), peak compressive strain (centre), and peak shearing strain (right) within the lamina cribrosa of the model reconstructed from the right eye of Donor 1. Input factor levels were scaled from minimum (−1) to

maximum (+1) values. See Fig. 1 for actual values and baseline levels. All cases correspond to an increase in IOP from 5 to 50 mmHg. Steep lines represent large factor effects on the outcome measure

material to effect of geometry for each of the 30 outcome measures.

By comparing the outcome measure response curves from the generic model with those from the individual-specific models we were also able to assess the physiologic relevance of the generic model. The response curve from a generic model should ideally be within the maximum and minimum outcome measure levels over all individual-specific models.

### 3 Results

To illustrate the effects of variations in material properties, Fig. 3 shows the peak levels of three modes of strain within the lamina cribrosa (LC) of one individual-specific model as the six input factors are changed. Increases in input factors, corresponding to stiffening of the tissues for the moduli and to a reduction in compressibility for the Poisson ratio, always produced a decrease in the peak strain within the LC, but the magnitude of the effect varied from one input factor to another. The effects of material variation were larger for more compliant materials, in agreement with results from generic models (Sigal et al. 2005a). Variations in scleral stiffness had the largest effect of all input factors. As discussed in detail in Sigal et al. (2007b, 2008), the highest strains occurred in compression, followed by shearing and finally by tension.

The absolute and total responses of all outcome measures for the same individual-specific model to variations in all input factors are shown in Fig. 4. The height of each bar represents the total response of an outcome measure due to variations in all input factors. This figure allows simultaneous evaluation of both the relative contribution of an input factor to the variations in an outcome measure (the absolute response) and the total response of the outcome measure to

independent variations in all input factors. The most influential outcome measure was the variation in scleral stiffness, accounting for approximately half all the effects.

#### 3.1 Comparison of responses between models

The effects of changing scleral stiffness is illustrated in Fig. 5, which plots median strain within the pre-laminar neural tissues for different models. The sensitivity of all models to variations in scleral stiffness is surprisingly similar. Predicted compressive strains are of a larger magnitude than tensile and shearing strains, and all are reduced as the sclera stiffens. Although different models overlap, the results from contralateral eyes are often close to each other. Figure 5 also illustrates the results obtained using the generic model based on Model 3 of Sigal et al. (2004), which clearly shows a similar response to that of the individual-specific models.

#### 3.2 Ranking of input factors

The total influence of all input factors over the ten outcome measures for each mode of strain are plotted in Fig. 6, for all the individual-specific models and the 3D generic model. Based on Fig. 6, the relative levels of influence were used to rank input factors. For all three modes of strain, and for all models, scleral stiffness was the most influential input factor, followed by lamina stiffness and the stiffness of the pia mater. The compressibility of the pre-laminar neural tissue had the smallest influence on tensile strains, as previously found (Sigal et al. 2005a). However, the influence of pre-laminar compressibility increased for shearing strains and even further for compressive strains.

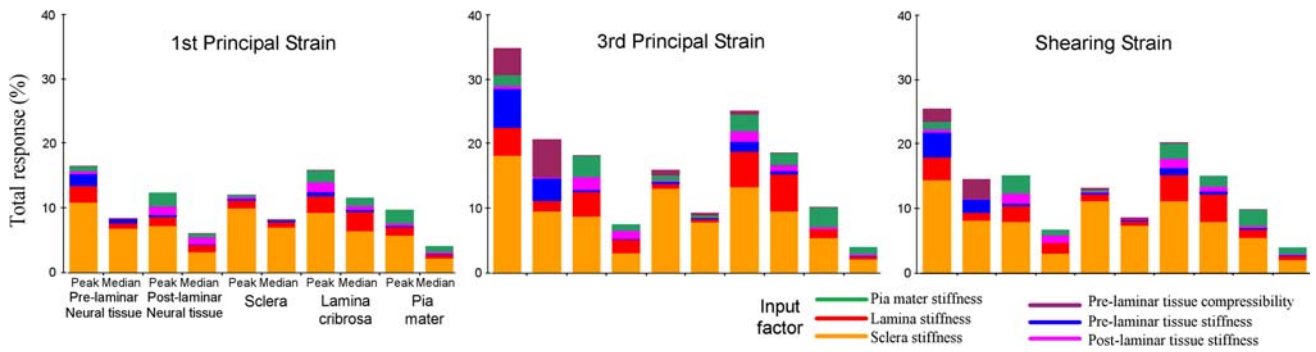


**Fig. 4** Response ranges of all outcome measures to variations in all input factors for the right eye of Donor 1. Outcome measures were grouped according to the mode of strain: first principal strain (*left*), third principal strain (*centre*) and maximum shearing strain (*right*). Each colour corresponds to one input factor (see colour legend at lower right), so that the height of each colour in the graph is proportional to the abso-

lute response of the outcome measure to that particular input factor. The total bar height represents the total outcome measure variation due to changes in all input factors. All factors are plotted; however, if their effect on an outcome measure was small the corresponding portion of the bar may not be easily distinguished

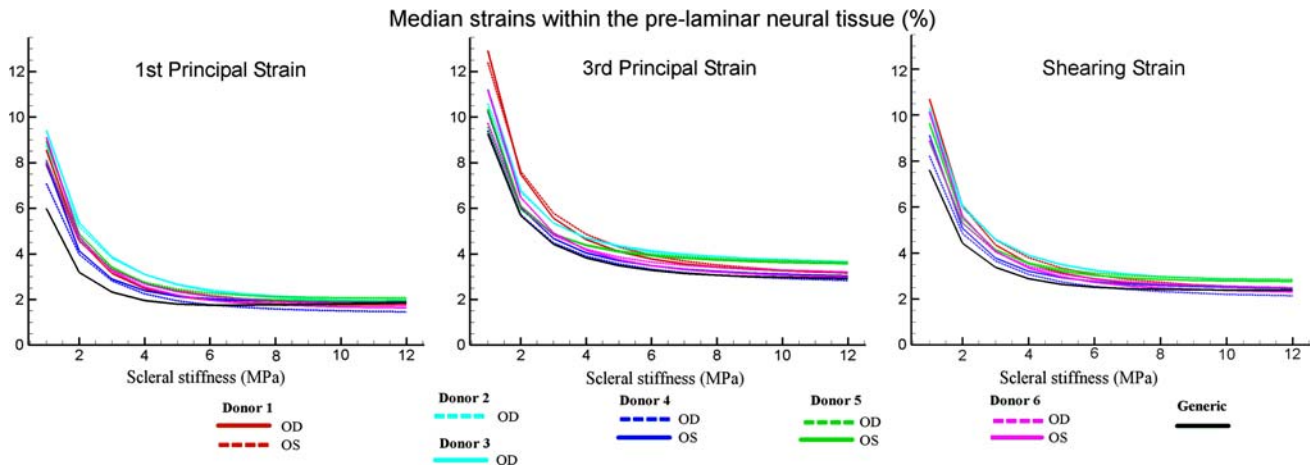


**Fig. 5** Effects of variations in scleral stiffness on median first principal strain (*left*), median third principal strain (*middle*) and median maximum shearing strain (*right*) within the pre-laminar neural tissues

of all individual-specific models (*coloured lines*) and a generic model (*black line*). All cases were for an increase in IOP from 5 to 50 mmHg. *OD* right eye; *OS* left eye

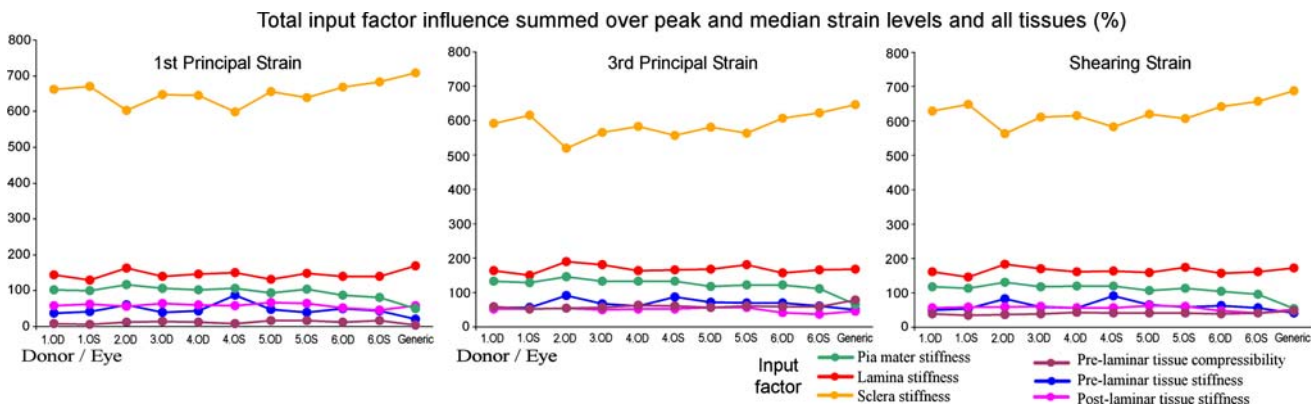


**Fig. 6** Total influences of all input factors computed for peak and median tensile strain (*left*), compressive strain (*middle*) and shearing strain (*right*) over all tissue regions for all models. Higher values represent larger influences of the input factor over the mode of strain for the

particular model. See Sect. 2 for the definition of the total influence of an input factor. In this graph, the plotted quantity is obtained by summing the peak and median strains over all tissue regions. *OD* right eye, *OS* left eye

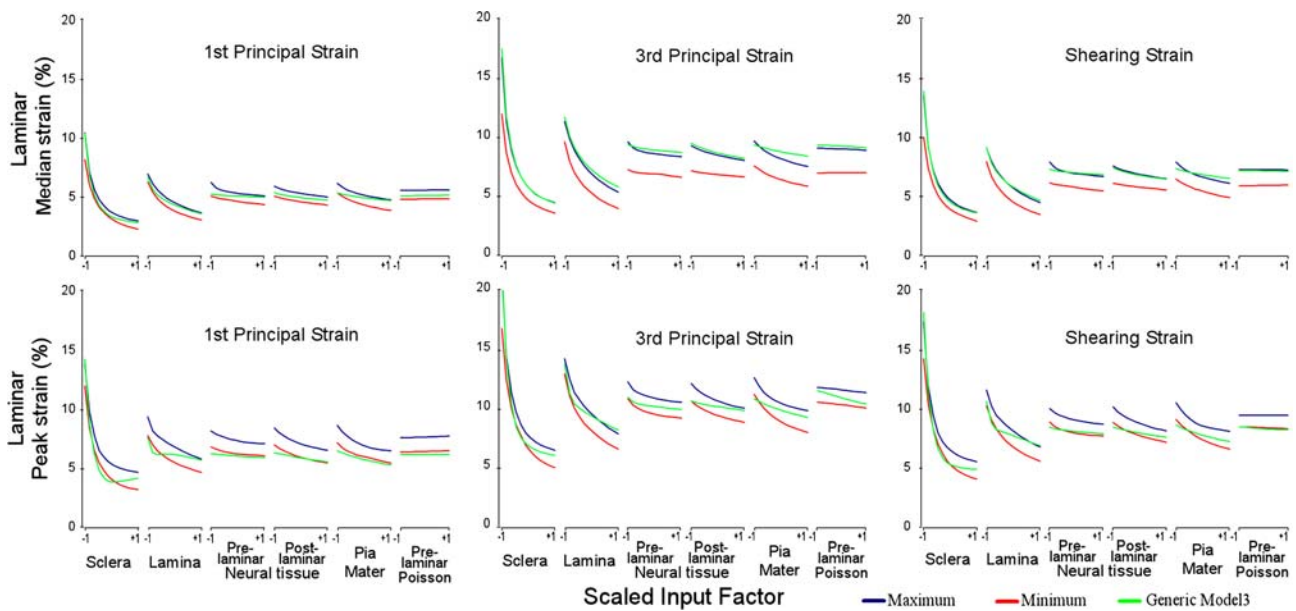


**Fig. 7** Sensitivity to variations in all input factors of six measures of strain within the lamina cribrosa: median (*top row*) and peak (*bottom row*) levels of first principal strain (*left column*), third principal strain (*centre column*) and shearing strain (*right column*). Within each panel, input factors were varied from the minimum (−1) to the maximum (+1) values. Input factors refer to the stiffness of each tissue, except pre-laminar Poisson that refers to the compressibility of the pre-lami-

nar neural tissue. A pair of lines representing the maximum (*blue*) and minimum (*red*) value of an outcome measure at each level, computed over all individual-specific models, are shown for each input factor and outcome measure combination. The responses of all individual-specific models are contained between these lines. The *blue* and *red* lines were used to compute the effect of geometry and the effect of material, as shown in Fig. 2

### 3.3 Effects of variations in geometry and materials : response envelopes

The extrema of the strain levels within the lamina cribrosa over all individual-specific models are shown in Fig. 7. The distance between blue and red lines shows the range of values due to the *effect of geometry* (see Fig. 2) and is larger in some outcome measures than in others. In general, variations in an input factor had little effect on the *effect of geometry*. As in Figs. 3 and 5, the slope of a line shows the influence on the outcome measure of variations in the input factor, which we have referred to as *effect of material* (see Fig. 2).

### 3.4 Ratio of effects of materials to effects of geometry

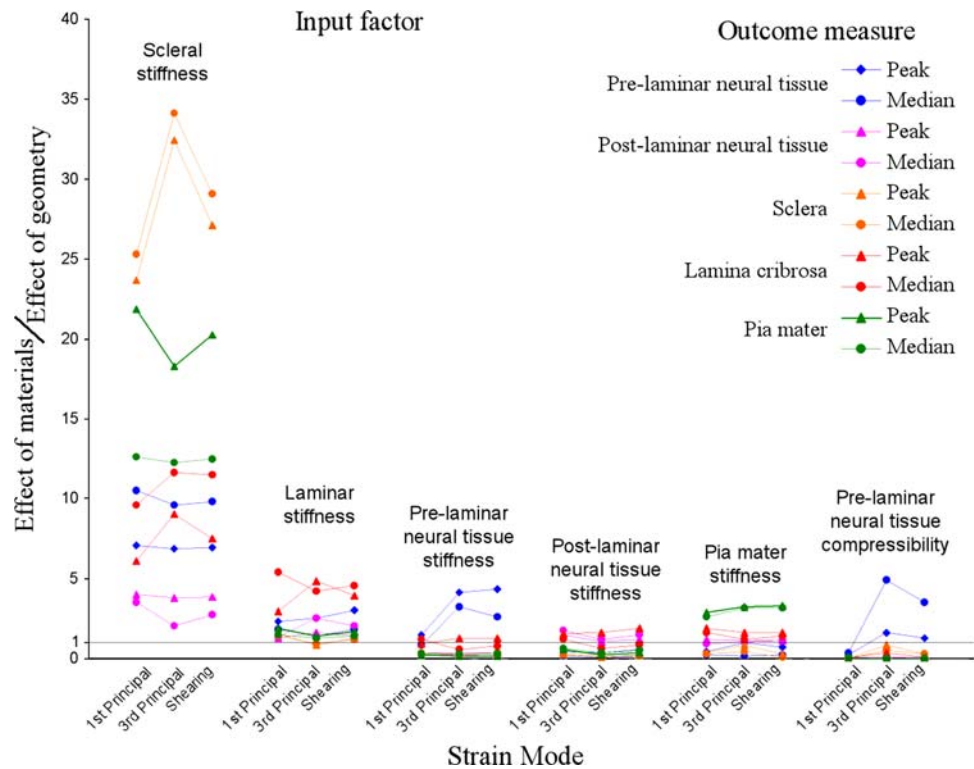
The ratio of effects of materials to effects of geometry are shown in Fig. 8. A large ratio represents an outcome measure that had larger changes due to variations in material properties than that due to geometry. For example, variations in scleral stiffness produce about 10 times more change in the median compressive strain within the pre-laminar neural tissue than differences in geometry. Generally, variations in scleral and lamina cribrosa stiffness had a larger effect than did changes in geometry (anatomy).

## 4 Discussion and conclusions

In this work we have described the results of a parametric analysis of the influences of mechanical properties and geometry on the mechanical response of an ONH to changes in IOP. This study is the first to consider individual-specific models of human ONHs in a sensitivity analysis, and to evaluate the relative effects of geometry and material properties. The main conclusions are that the stiffness of the sclera is the most influential input factor in ONH biomechanics (Fig. 6), and that differences in geometry often had a smaller effect in ONH biomechanics than variations in material properties (Fig. 8). These conclusions are robust in the sense that input factor rankings were remarkably consistent from one individual-specific model to another.

Unlike our previous work using generic models, where the geometry of the ONH could be varied parametrically, the use of individual-specific 3D geometries necessitated some special considerations. Specifically, the influences of material and geometric input factors had to be analysed separately. While material properties could be varied continuously, the individual-specific geometries formed a discrete, unordered dataset that we take as representative of the larger set of physiologically occurring ONHs. Hence the sensitivity to material properties was analysed using systematic variations in

**Fig. 8** Ratio of the effect of materials to the effect of geometry for all input factors and outcome measures computed as shown in Fig. 2. Values above 1 indicate that variations in input factor level, i.e. material properties, produce larger effects than differences in geometry between models. Each set of three points represents the effects of changing one input factor (see label above points) on a single outcome measure, as listed in the legend at top right



the biomechanical properties (Sigal et al. 2005a), while the sensitivity to geometry was defined by comparisons between our discrete set of individual-specific models.

When the deformation of the ONH was modeled using baseline material properties, the differences in predicted response between models were minor (Sigal et al. 2008), suggesting a small influence for the geometry in the ONH biomechanical environment. The results presented herein confirm these results and extend the conclusions beyond the baseline set of material properties. In particular, the variation in outcome measure between individual-specific models was only weakly dependent on input factor values, further confirming the dominance of material properties over geometric features in determining the acute response of the ONH to IOP.

For all cases other than for a very stiff sclera, the predicted strain levels reached levels that have been shown to have biological effects on other systems. However, the exact mechanisms by which strain is transduced into a physiologic effect are not well understood and it is still unclear which modes and magnitudes of strain are of physiologic relevance. Please see the companion paper Sigal et al. (2008) and Sigal (2006) for more details.

We have previously used generic (non-individual-specific models) to analyse ONH biomechanics (Sigal et al. 2004, 2005a,b), and it is of interest to evaluate how the results of this work compare to studies with generic models. Both our main conclusions are in agreement with our previous predictions using generic models (Sigal et al. 2005a). Moreover, specific

predictions obtained from the reconstructed ONH based on the generic model [used for analyses in Sigal et al. (2005a)] were similar to those obtained with the individual-specific models. There were some differences: for a few outcome measures the generic model led to over- or under-predictions of strain (Fig. 8). It is also evident the differences between median and peak values are less in the generic models than in the individual-specific models (Fig. 8). One possible explanation for this is insufficient refinement of the 3D generic model. The number of elements required in the 3D models (generic or individual-specific) was determined through the mesh refinement analysis previously described (Sigal et al. 2005b). Insufficiently refined models appear “stiffer” and more homogeneous, giving predicted levels of strain that are lower and more homogeneous from one tissue region to another (Cook 1995). A larger ROI was reconstructed for the generic model than for the individual-specific models [Table 2 in Sigal et al. 2008], resulting in a larger mean element length in the generic models (Fig. 6). However, there were no cases where the predictions from generic models were more than a few percentage points of strain away from the range of individual-specific models. This confirms that many of the conclusions derived from the generic axisymmetric models presented in Sigal et al. (2004, 2005a) extend to individual-specific models as a good first approximation.

Previous work using generic models identified the stiffnesses of the lamina cribrosa and pia mater as the second and third most influential material input factors, a result that was

confirmed here using individual-specific models. However, in the studies on generic models, little attention was given to the importance of the stiffness of the pia mater and the compressibility of the pre-laminar neural tissue, mostly because they were overshadowed by the input factors related to geometry. It is possible that some of the increased influence of the pia mater that we observed in individual-specific models was due to the pia's enlarged volume compared with generic models. This increased volume came about through the iterative process of model reconstruction (Sigal et al. 2005b; Sigal 2006), which was designed to produce models with a continuous pia mater that retained its structural integrity, and that when meshed could be analysed accurately using the finite element method. This meant that the pia mater thickness in the individual-specific models was sometimes slightly larger than in the histological sections and in the generic models, likely producing a non-physiologic increase in flexural rigidity that amplified the influence of the pia mater.

The pia mater is relatively thin, even when compared with other ONH structures; nonetheless, we believe that the pia mater could play a mechanical role in the ONH similar to that identified for the spinal cord: it increases the effective stiffness of the neural tissues and stores elastic energy during acute deformations, improving shape recovery. For example, Ozawa et al. (2004) studied the effects of the pia mater on the mechanical response of rabbit spinal cord by comparing measurements in cords with an intact pia mater with others where the pia mater had been incised at both sides. They found that an intact pia mater tripled the modulus of the spinal cord from  $5 \pm 2$  to  $16 \pm 5$  kPa, and that the shape of spinal cord specimens with an intact pia mater were well restored after removal of compression, whereas those with an incised pia mater remained deformed. They measured a pia mater modulus of elasticity of 2.3 MPa, about 460 times that of the neural tissue, a property they attributed to its highly fibrous structure. Henderson et al. (2005) and Tunturi (1978) observed similar effects in the canine spinal cord. Future improvements in the simulations could model the pia mater using shell elements, so that no artificial increase in thickness is required, while still maintaining structural integrity.

The compressibility of the pre-laminar neural tissue was found to be more influential in ONH biomechanics than predicted in previous studies. This was because previous studies restricted attention to tensile strains (first principal strain), precisely the mode of strain that we observed to be least affected by compressibility. For compressive (third principal) and shearing strains, the influences of compressibility were several times larger, and although still much smaller than those of sclera, lamina and pia mater stiffness, about as influential as neural tissue stiffness. Significant effects of compressibility in the sensitivity of tissues to forces have been observed before, for example in cartilage where poroelastic effects increased strain by up to an order of magnitude.

Note that as defined in this work, the magnitude of the maximum shear strain has to be intermediate between the first and third principal strains, and is therefore not an independent measure of strain. However, we have included plots of this quantity for reasons described in the companion paper (Sigal et al. 2008).

#### 4.1 Limitations

The simulation studies described in this work were subject to several limitations in addition to those discussed above. The virtues and limitations of the techniques used in these studies have been presented in detail elsewhere (Sigal et al. 2005a,b, 2007a,b; Sigal 2006). In summary, the process of finite element analysis requires the definition of geometry, boundary conditions and material properties. Each of these steps necessitated approximations that could influence both the numerical and physiological accuracy of the predictions. The quality of model geometry was analyzed in Sigal et al. (2005b) and Sigal (2006). The application of boundary conditions, in particular the use of the same generic axisymmetric shell model for all individual-specific models, also likely plays an important role. This could be particularly important given the large influence of scleral properties. The use of linear material properties that do not explicitly consider the micro-structure of the ONH, particularly the lamina cribrosa, are potentially relevant (Sigal et al. 2004) and could influence the choice of acceptable ranges for the moduli of elasticity (Sigal et al. 2005a).

As mentioned in Sect. 2, unfortunately the range of physiologically reasonable values is unknown. The choice of ranges and baseline configuration could potentially influence the results. An unnaturally large range for a tissue could make the tissue artifactually influential and conversely make other tissue influences artifactually modest. We tried to reduce the arbitrariness of the results by varying the Young's modulus of all tissues over the same proportional ranges (one-third to four times the baseline level). For all Young's modulus the effects of variations were larger for more compliant cases. Which implies that having a higher upper limit for the material ranges would not have had a substantial impact on the results. This is important as experimental technique limitations have led previous authors to report "upper boundary" measures of tissue modulus (Downs et al. 2003, 2005; Spoerl et al. 2005). Hence, it is potentially more critical to identify the lower boundary of the measures. For a more detailed discussion on the choice of material property values and ranges, and possible consequences on the responses predicted with the simulations please refer to Sigal et al. (2004, 2005a) and Sigal (2006).

All the studies on scleral mechanical properties included in Fig. 1 have been carried out using uniaxial tests, with the exception of Woo et al. (1972). This is important as uniaxial

tests on soft tissue often produce moduli substantially different to those from biaxial testing (Cook 1995). Woo's reported scleral modulus was 2.3 MPa well within the range considered in this study. In addition, most of the studies, including Woo's, were carried out at levels of strain that were more appropriate for impact studies rather than to IOP-induced deformations. Analytical and numerical models (Sigal et al. 2005a, 2007b; Sigal 2006) suggest that IOP-induced scleral strains produced by an increase in IOP of 45 mmHg are unlikely to exceed 3–5%. Yet experiments on scleral mechanics have studied scleral properties at strain levels of 8% (Spoerl et al. 2005), 20% (Downs et al. 2005; Friberg and Lace 1988), and up to failure (Downs et al. 2005; Uchio et al. 1999). If higher scleral moduli had been used in this study, then lower scleral strains would have been predicted, further pushing the high strain experiments outside of the relevant range. At high levels of strain most studies also found a nonlinear scleral response, where the stiffness increased with strain. But interestingly, even at 20% strain Friberg and colleagues (Friberg and Lace 1988) reported a modulus of  $1.8 \pm 1.1$  MPa, well within the ranges of our work. This is perhaps due to their use of uniaxial tests. Clearly there is a large range in the reported values of scleral moduli in the peer reviewed literature. Some of this variation is due to the experimental technique, but some is due to inhomogeneity between samples or between individuals. The combination of high uncertainty with the high sensitivity suggested by numerical models discussed above is a major problem, and is one of the reasons we have carried out the present study.

Besides linearity, other important assumptions regarding the mechanical properties of the ONH tissues are isotropy and homogeneity. These assumptions likely influence the model responses, and incorporating improved mechanical properties is at the center of our current research efforts (Eilaghi et al. 2007; Olesen et al. 2007). Our preliminary results on scleral inhomogeneity show that the modulus of the sclera varies significantly over the globe, and that the sclera is more compliant near the ONH. Some studies have reported an anisotropic scleral response, most notably Battaglioli and Kamm (1984), who found a sclera that is 100 times more extensible across the shell (radially) than along the shell (tangentially). Recent computational models have used these results to estimate changes in globe volume due to intravitreal injections (Kotliar et al. 2007). However, the paucity of information regarding the mechanical behaviour of the tissues of the ONH, and the difficulties in producing relevant experimental data are not to be underestimated (Humphrey 2006). Assuming more complex properties without reasonable estimates of the true physiologic ranges makes the models more complicated, not necessarily more realistic.

All the eyes were assumed to be healthy and non-glaucomatous. Considering the donor ages it is possible that some had undiagnosed eye problems or conditions

not reported to the eye bank. Some studies have found a positive correlation between scleral modulus and donor age (Spoerl et al. 2005). Future computational studies with an interest in incorporating individual-specific material properties might then use higher moduli, or a higher moduli range, when modeling older eyes.

The individual-specific models used did not consider the vascular tree within the ONH. We have previously determined that a simplified central retinal artery had limited effect in ONH biomechanics (Sigal et al. 2004), but the effects of more complex vasculature should be further studied.

Another limitation of the individual-specific models is that they have not been completely validated. Comparison of model predictions with measurements obtained with the HRT (Sigal et al. 2004, 2005b, 2008), suggest a general agreement in IOP-induced deformation of the vitreo-retinal interface. However, the degree of agreement varies considerably from eye to eye, as discussed in more detail in the companion manuscript (Sigal et al. 2008).

## 5 Conclusion

Material properties of ONH tissues play a dominant role in the mechanical response of an ONH to acute changes in IOP. In particular, the stiffness of the sclera was found to have a much larger influence than the stiffness of any other ONH tissue. Also influential were the stiffnesses of the lamina cribrosa and pia mater. These results are consistent with those predicted using generic models. The compressibility of the pre-laminar neural tissue was again found to have no influence on tensile strains, but was found to influence compressive and shearing strains. We remind the reader that these results apply only to the acute response of ONH tissues (not to long-term remodeling) and that the levels or distributions of strain needed to induce a biological response in cells of the ONH are unknown.

**Acknowledgments** This work was supported by the Consejo Nacional de Ciencia y Tecnología de México (IAS), the Canadian Institutes for Health Research (CRE, JGF), the Canada Research Chairs Program (CRE) and Glaucoma Research Society of Canada. We thank the Eye Bank of Canada for providing donor tissue.

## References

- Battaglioli JL, Kamm RD (1984) Measurements of the compressive properties of scleral tissue. *Invest Ophthalmol Vis Sci* 25(1):59–65
- Cook RD (1995) *Finite element modeling for stress analysis*. Wiley, New York
- Downs JC, Suh JK, Thomas KA, Bellezza AJ, Burgoyne CF, Hart RT (2003) Viscoelastic characterization of peripapillary sclera: material properties by quadrant in rabbit and monkey eyes. *J Biomech Eng* 125(1):124–131

- Downs JC, Suh JK, Thomas KA, Bellezza AJ, Hart RT, Burgoyne CF (2005) Viscoelastic material properties of the peripapillary sclera in normal and early-glaucoma monkey eyes. *Invest Ophthalmol Vis Sci* 46(2):540–546
- Edwards ME, Good TA (2001) Use of a mathematical model to estimate stress and strain during elevated pressure induced lamina cribrosa deformation. *Curr Eye Res* 23(3):215–225
- Eilaghi A, Sigal IA, Olesen CG, et al (2007) The effect of nonlinear scleral properties on optic nerve head biomechanics. Summer bioengineering conference 2007. Keystone, Colorado
- Friberg TR, Lace JW (1988) A comparison of the elastic properties of human choroid and sclera. *Exp Eye Res* 47(3):429–436
- Henderson FC, Geddes JF, Vaccaro AR, Woodard E, Berry KJ, Benzel EC (2005) Stretch-associated injury in cervical spondylotic myelopathy: new concept and review. *Neurosurgery* 56, 5, 1101–1113; discussion 1101–1113.
- Humphrey JD (2006) Cardiovascular solid mechanics. Springer, Heidelberg
- Kotliar K, Maier M, Bauer S, Feucht N, Lohmann C, Lanzl I (2007) Effect of intravitreal injections and volume changes on intraocular pressure: clinical results and biomechanical model. *Acta Ophthalmol Scand* 85(7):777–781
- Olesen CG, Tertinegg I, Eilaghi A, et al (2007) Measuring the biaxial stress-strain characteristics of human sclera. Summer bioengineering conference 2007. Keystone, Colorado
- Ozawa H, Matsumoto T, Ohashi T, Sato M, Kokubun S (2004) Mechanical properties and function of the spinal pia mater. *J Neurosurg Spine* 1(1):122–127
- Sigal IA, Flanagan JG, Tertinegg I, Ethier CR (2004) Finite element modeling of optic nerve head biomechanics. *Invest Ophthalmol Vis Sci* 45(12):4378–4387
- Sigal IA, Flanagan JG, Ethier CR (2005a) Factors influencing optic nerve head biomechanics. *Invest Ophthalmol Vis Sci* 46(11):4189–4199
- Sigal IA, Flanagan JG, Tertinegg I, Ethier CR (2005b) Reconstruction of human optic nerve heads for finite element modeling. *Technol Health Care* 13(4):313–329
- Sigal IA (2006) Human optic nerve head biomechanics: an analysis of generic and individual-specific models using the finite element method. Department of Mechanical and Industrial Engineering, University of Toronto, Toronto
- Sigal IA, Flanagan JG, Ethier CR (2007a) Interactions between factors influencing optic nerve head biomechanics. Summer Bioengineering Conference 2007. Keystone, Colorado
- Sigal IA, Flanagan JG, Tertinegg I, Ethier CR (2007b) Predicted extension, compression and shearing of optic nerve head tissues. *Exp Eye Res* 85(3):312–322
- Sigal IA, Flanagan JG, Tertinegg I, Ethier CR (2008) Modeling individual-specific human optic nerve head biomechanics. Part I: IOP-induced deformations and influence of geometry. *Biomechan Model Mechanobiol* (doi: [10.1007/s10237-008-0120-7](https://doi.org/10.1007/s10237-008-0120-7))
- Spoerl E, Boehm AG, Pillunat LE (2005) The influence of various substances on the biomechanical behavior of lamina cribrosa and peripapillary sclera. *Invest Ophthalmol Vis Sci* 46(4):1286–1290
- Tunturi AR (1978) Elasticity of the spinal cord, pia, and denticulate ligament in the dog. *J Neurosurg* 48(6):975–979
- Uchio E, Ohno S, Kudoh J, Aoki K, Kisielewicz LT (1999) Simulation model of an eyeball based on finite element analysis on a supercomputer. *Br J Ophthalmol* 83(10):1106–1111
- Woo SL, Kobayashi AS, Schlegel WA, Lawrence C (1972) Nonlinear material properties of intact cornea and sclera. *Exp Eye Res* 14(1):29–39